Mechanical Metamaterials

Final Report

By

Brent Peluso
bpeluso@calpoly.edu

Oliver Parker
oparker@calpoly.edu

Mechanical Engineering Department

California Polytechnic State University, San Luis Obispo

March 2023

Prepared For:

Professor Long Wang

Civil and Environmental Engineering Department

Abstract

Mechanical metamaterials are an emerging design strategy aimed at tailoring lattice structures to achieve specific properties such as negative Poisson's ratios and guiding wave propagation. These metamaterials have received increasing attention from various application domains, including medical devices, aerospace, automobile, and infrastructure. The scope of this project is to vary a single lattice parameter and quantify its effect on the structural properties of the given 3D lattice. This document contains the results of the preliminary design process, including background research, project definition/scope, concept creation and selection, and general timeline.

Table of Contents

1. Introduction

Mechanical metamaterials is a broad term used to describe a range of three-dimensional structures whose engineering properties are a product of their structure rather than the inherent properties of the base material. Advantages of metamaterials structures extend to structural, electromagnetic, optical, and acoustic applications, among others. To contribute to the breadth of the emerging field of metamaterials research, this project aims to evaluate and document the effects of varying an individual lattice parameter on the overall mechanical properties of the structure. This document includes background information collected from existing publications, the key goals of our work, our concept creation/selection procedures, and the process and general timeline followed to satisfy the project objectives.

2. Background

2.1 Interview with sponsor

To best understand the scope of this project, a meeting with our sponsor, Dr. Wang, was conducted. Dr. Wang has research interests in metamaterials, and in particular lattice structures, and so, he would like the ability to tailor a structures specific properties based on the lattice design used to build said structure. Due to the open-ended nature of this project, certain refinements needed to be made so as to be completable in a year, without prior extensive knowledge on lattice structures. In collaboration with Dr. Wang, our team decided that the goal would be to build an array of lattice structures all stemming from the same core design, through the varying of a build parameter such as strut design, or nodal placement, to better understand the impact of certain design choices. Additionally, these structures will be 3D printed and mechanically tested to determine performance.

2.2 Lattice generation

Lattice generation was one of the first challenges our team encountered when starting this project. From our literature review, there are several ways lattices are generated, but the main two are as follows, CAD software [1] or Python/MATLAB code [2]. Both options have validity, and depending on the application, will be more or less convenient for the user.

When it comes to code base generation, there are user made addons to MATLAB such as MSLattice [3] with an interface where parameters are input by the user, and a lattice is automatically generated from a general database of different unit cells. The interface for the MATLAB program MSLattice is shown in Figure 1. This is quite a convenient method as it requires very little work to build lattice structures with changing relative densities or sizes. However, it does not allow for full control over the structure parameters our team would like. Design changes such as moving the nodal location or changing the strut design are still currently unavailable. Additionally, only specific lattices can be built using these programs, which limits the design choices our team has.
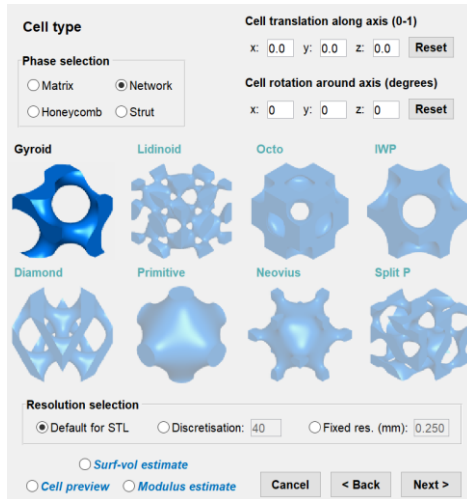
Figure 1. MSLattice unit cell generation interface

The other option in code-based generation is for our team to write its own lattice generating script in either MATLAB or Python. Initially a wire frame is built, seen in Figure 2 [], then the struts are given mass through matrix manipulation. This currently is not the route the team plans on taking, as coding is neither of our strong suits, but may be readdressed later if need be.
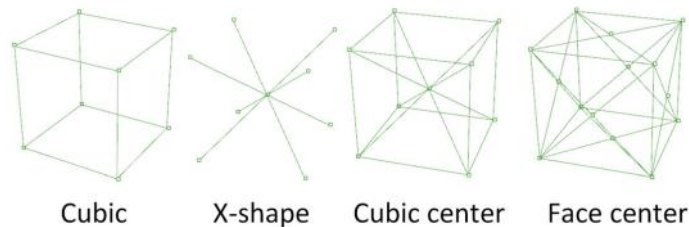

Figure 2. Wire frame models of lattice structures build through code

The second option for lattice generation is CAD based software. There are advantages to using CAD software for lattice generation, particularly, the startup time required to get initial structures designed. While it may take many weeks to understand and be able to generate our own code to build lattices, models could immediately begin to be generated using CAD software. CAD software has been shown to have the capabilities to build complex 3D lattice unit cells, and making use of liner patterns, lattice structures can be generated [1].

Although it has been reported that CAD tools are inefficient when it comes to generating large lattice structures, as they generate large files and require high RAM usage [1], for the applications of the project, this appears to be the better solution. The goal of this work is not to optimize an internal structure with complex geometry with lattices or to generate a continually changing lattice, but simply to understand the effects of design choices on a uniform cubic lattice structure. Because of this, the high computing cost should not be a major barrier to overcome.

2.3 Unit cell

Unit cell section for lattice generation is a crucial design choice that affects the mechanical properties of the structure. In terms of lattice structures, there are two main deformation or failure modes that are observed, stretch or bending dominated, which can be determined though a set of criteria, specifically the Maxwell criterion. In this criterion, Maxwell defined a variable M seen in equation (1).

$$M = s - 3n + 6$$

Here, s is the number of struts in the unit cell, and n is the number of nodes. For M < 0, there are not enough struts to equilibrate the external forces on the structures without including bending moments at the nodes. Because of this, structures with M < 0 are defined as bending dominated structures. On the other hand, when M ≥ 0, the axial tension and compression in the struts can equilibrate external loads, and little or no bending occurs at the nodes, creating stretch dominated behavior [5]. While this criterion lays the foundation for what to expect when building and testing lattice structures, it is not an exact science, and some structures which are categorized as stretch or bending dominated, may perform differently.

Generally, a structure that is defined as being stretch dominated is stiffer and stronger per unit weight than a structure dominated by bending, with a higher modulus and initial yield strength. Based on the application of the part, either could be desirable, with stretch-based lattices being used for low weight high strength applications, and bending dominated structures more typically being used for energy absorption applications [4].

3. Objectives

This project is largely, if not entirely, research oriented. While product specifications exist, much of this work aims to analyze and classify the effects of varying a specific lattice parameter. As such, some specifications, such as unit cell weight or compression testing, do not have specific targets or tolerances. Yet, completion of these specifications is integral to the success of this project. Table 3.1 provides a complete list of key specifications.

3.1. Problem Statement:

The problem statement for this project is given as follows: Mechanical metamaterials is an emerging design strategy aimed at tailoring lattice structures to achieve specific material properties. The metamaterials field of research is limited and needs research classifying how varying individual lattice parameters impacts material properties.

3.2. Stakeholder Wants/Needs:

The main stakeholders are Dr. Wang, future members of Dr. Wang's research team developing on this work, as well as the larger metamaterials field of research. These stakeholders are looking for organized information classifying the changes in properties of lattice structures, such as stiffness and energy absorption, as a result of altering a specific lattice parameters. Further, the stakeholders are seeking a replicable modeling and manufacturing process for the creation of high-resolution 3D printed lattice structures.

Table 3.1. Specifications Table

Spec #	Specification	Requirement/Target	Tolerance	Risk	Compliance
1	Finite Element Analysis	Compressive Stress Distribution	N/A	H	I
2	Overall Lattice Print Size	14.5x14.5x18.5 cm	Max	H	A
3	Time to Print Lattice	One day	Max	L	A,I
4	Time to Model Unit Cell in CAD	1 hour	± 30 min	M	I
5	Compression Test	To Failure	N/A	H	T
6	Overall Lattice Densities	0.15, 0.20, 0.25 g/cm^3	N/A	H	T

The finite element analysis will evaluate the compressive stress distribution to provide initial insights into the failure modes of the unit cells of interest. Overall lattice print size is limited by the build platform size of the Formlabs Form 3B SLA 3D printer. Individual lattices will measure approximately 5cm x 5cm x 5cm, so this build platform can accommodate multiple simultaneous prints. One day maximum print time allows for a daily print schedule. Prints can run unattended. The lattice weight will be a function of its strut thickness and strut shape. This project will vary each of these parameters in order to examine their effects on lattice material properties. As such, the experimental nature of this process necessitates that lattice weight be documented, but no specific value or maximum is targeted as is often observed in consumer products.

4. Concept Design

Given the research-oriented nature of this project, the concept design took on a unique form when compared to traditional product-oriented ideation. The overall objective was to isolate two unit cells for which to study the effects of varying strut thickness and shape: one stretch-dominated structure and one bending-dominated structure.

4.1 Concept Development/Ideation

The initial stage of the concept design phase was the creation of multiple concepts. Each of the two group members independently produced five lattice structures for consideration. Tables
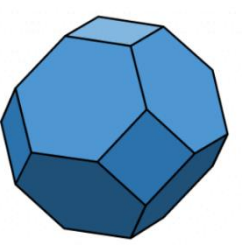
4.1(a) and 4.1(b) show these lattices in initial go/no-go matrices, an engineering judgment-based step of idea elimination.

Table 4.1(a). Brent's concept models in a go/no-go matrix.

☒	☑	☑	☑	☒
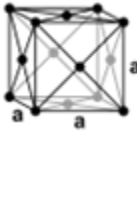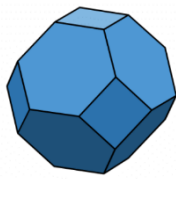
Table 4.1(b). Oliver's concept models in a go/no-go matrix

☑	☒	☒	☒	☑
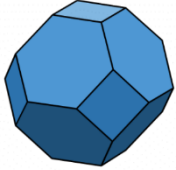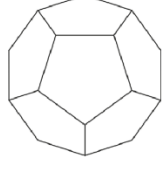
4.2 Pugh and Weighted Decision Matrices

The lattices from the go/no-go matrices above with check marks were scored in the Pugh matrix of Table 4.2 based on the design specifications. This phase of concept design was also performed by each group member individually.

Table 4.2. Pugh Matrix.

Design Criteria						
Time to Print	Datum	S	S	S	S	S
Time to Model		S	-	-	S	-
Printability (No internal supports)		S	S	+	S	S
Favors Single Stress Mode (Stretch or Bending)		-	+	+	+	S
ΣS		3	2	1	3	3
Σ+		0	1	2	1	0
Σ-		1	1	1	0	1
Total		-1	0	+1	+1	-1

Table 4.3. Weighted Decision Matrix.

Specification	Weight	Idea 1	Idea 2	Idea 3	Idea 4	Idea 5
Minimizes Print Time	1	4	4	2	4	4
Minimizes Modeling Time	2	2	2	2	1	3
No Internal Supports	4	3	3	4	2	2
Favors Single Stress Mode (Stretch or Bending)	4	1	5	5	4	2
Total		24	40	42	30	26

The Pugh matrix and weighted decision matrix facilitated the isolation of one unit cell for each mode of stress distribution: bending and stretching. Idea 4, a dodecahedron, was added for consideration as a bending-dominated cell but was ultimately eliminated largely due to CAD modeling complications as a result of a lack of symmetry.

4.3 Final Concepts

The weighted decision matrix of Table 4.3 highlights the final selected unit cells. Idea 2, the Kelvin cell shown in Figure 4.3(a), is selected as the bending-dominated structure of interest. Idea 3, the octet truss shown in Figure 4.3(b), is selected as the stretch-dominated structure of interest. Each of these cells favor a single mode of stress distribution and can be reliably printed without internal supports. As can be seen by their scores in Table 4.3, these cells are not the fastest to model when compared to other simpler structures. The importance of modeling time falls well below the importance of stress mode favoring and printing without internal supports. This is reflected in the weights assigned to each specification.

7
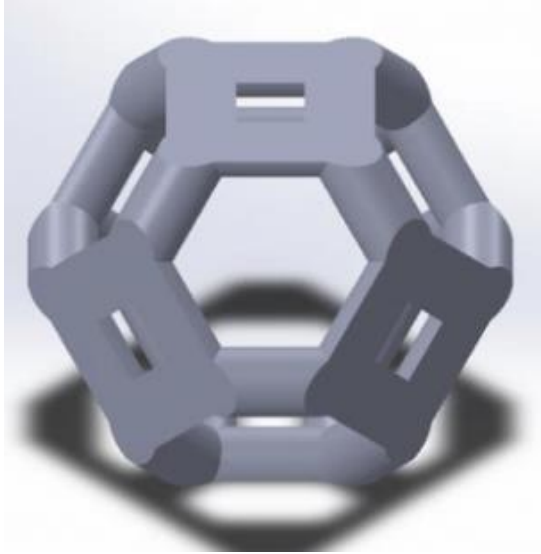
Figure 4.3(a). Kelvin Cell
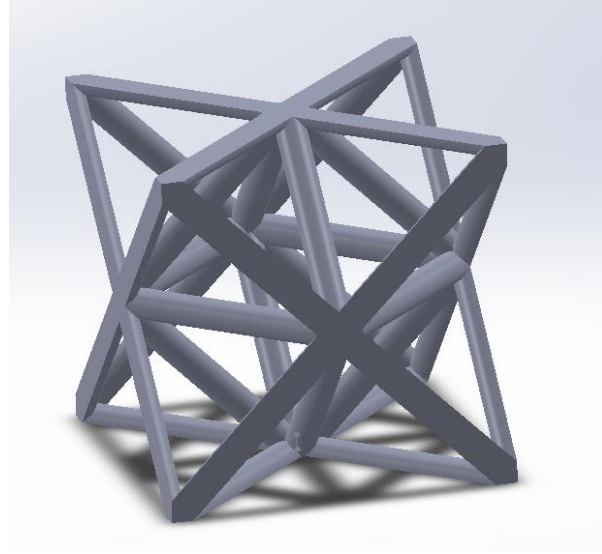
Figure 4.3(b). Octet Truss

4.4 Design Direction: Varying Strut Design

The two unit cells depicted in Figures 4.3(a) and 4.3(b) serve as the unit from which a full lattice will be generated. This project explores the effects of varying strut thickness and design. An example of this is the octet truss shown in Figure 4.4. Final lattice designs are discussed extensively in section 5 of this report.
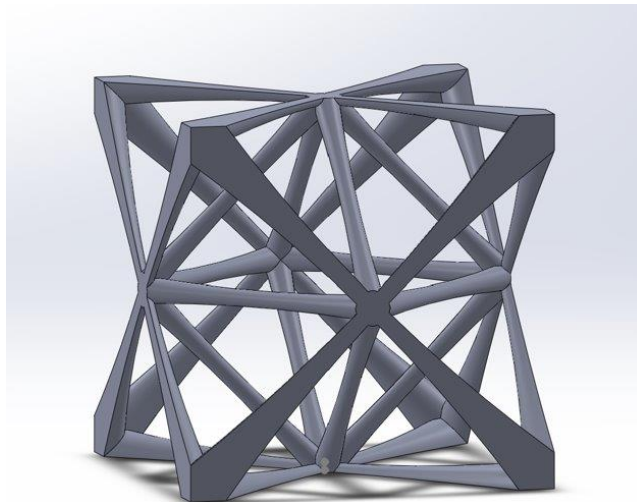
Figure 4.4. Octet truss with altered strut geometry.

4.5 Preliminary Design Risks

Before beginning the SLA 3D printing, the hazards of the manufacturing process and design were considered. These are documented in the design hazard checklist contained in Appendix D. Although the lattice structures themselves lack any notable hazards, the SLA 3D printing process carries a few hazards. Contact of the skin or eyes with the liquid resin can cause irritation and should be avoided by wearing gloves and safety glasses. Isopropyl alcohol should not be used to clean resin off skin if contact does occur, as it is a solvent and will speed absorption. The other main risk is the use of isopropyl alcohol (IPA) in large quantities in the washing stage of the 3D printed parts. IPA is a highly volatile, flammable, noxious substance that should be handled with gloves and safety glasses.

The team received a virtual training session from a Formlabs representative on May 19, 2022 prior to beginning printing. This session encompassed the features and operations of the Form 3B printer, including safe printing protocol.

The compressive testing phase of this project also poses a moderate safety risk to the Instron operator. These parts are rigid plastic and project at high speeds during fracture. The members of the team were trained on proper Instron universal testing operation by DR. Harding of the MATE department on October 28, 2022. Adequate PPE, including safety glasses and long pants/sleeves, is also necessary for safe compressive testing.

5. Final Design

The final unit cell designs to be fabricated for testing are detailed in this section. Ultimately, 10 unique lattice designs will be printed and tested. The details of each cell design are discussed below.

5.1 Final Lattice Designs

Because the objective of this project is to classify the compression testing outcome as it relates to both strut shape and lattice material density, both parameters are varied across the test specimens in isolation. As such, for both bending- and stretch-dominated cells, the three strut geometries, depicted in Figures 5.1(a) and 5.1(b), have been implemented. In addition, the cylindrical strut lattice is tested at two additional lattice densities. In total, there are 10 unique lattice models. The model drawings for each are included in Appendix G.
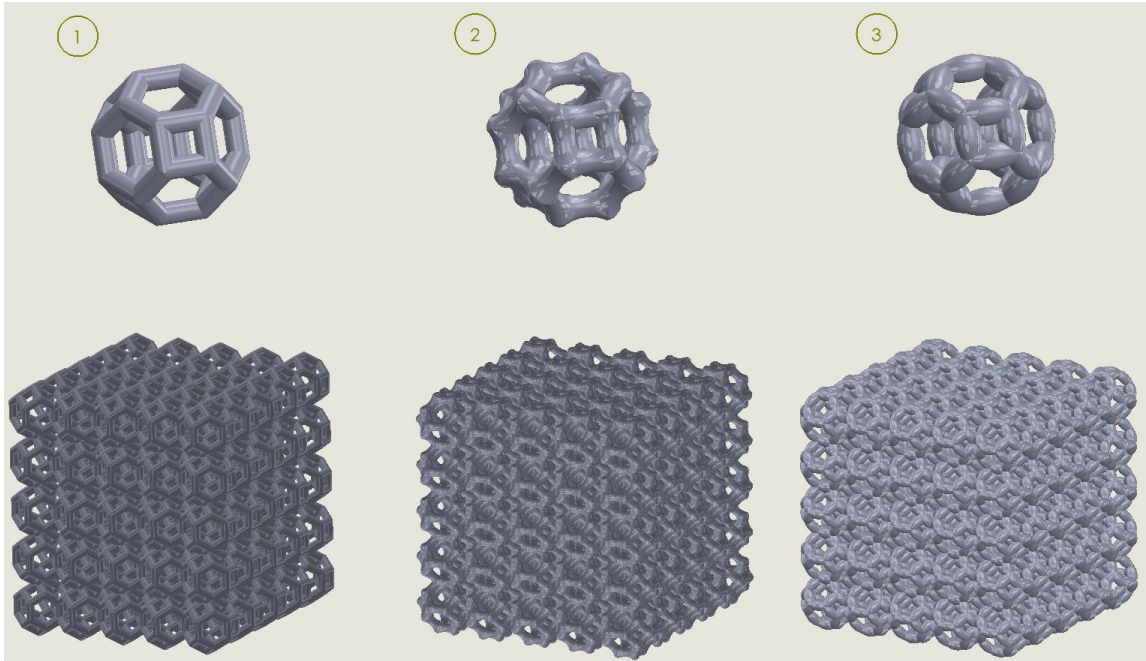
Figure 5.1(a). Kelvin Cell (bending-dominated) unit cell and lattice models for the three strut geometries: (1) cylindrical, (2) dog bone, (3) reverse dog bone.
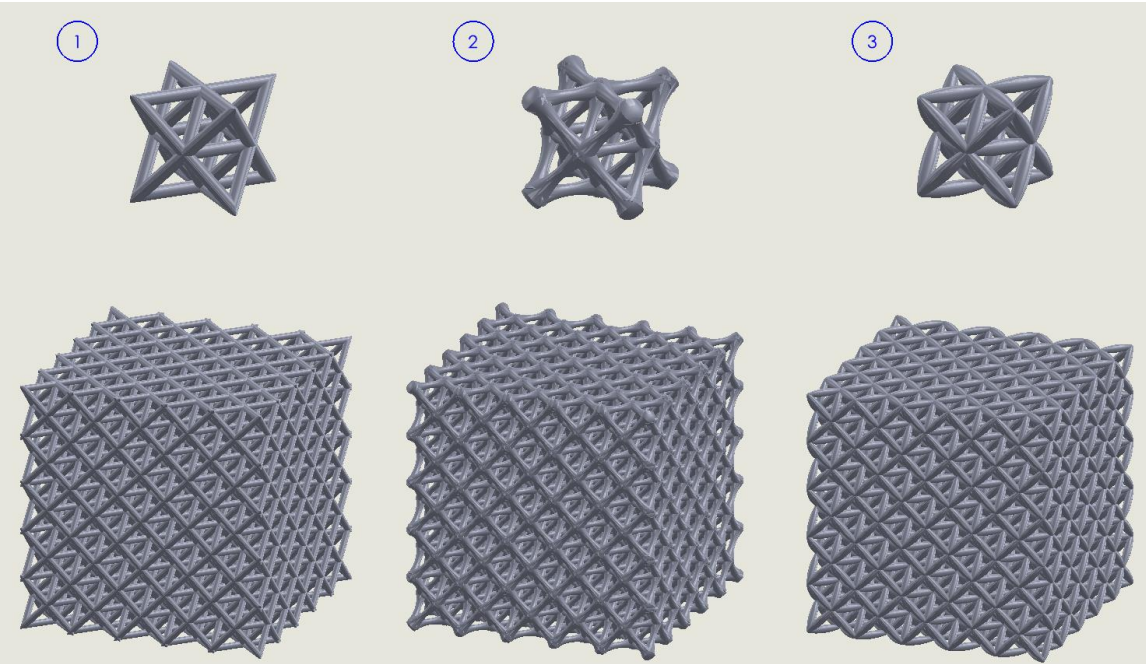
Figure 5.1(b). Octet Truss (stretch-dominated) unit cell and lattice models for the three strut geometries: (1) cylindrical, (2) dog bone, (3) reverse dog bone.

5.2 Structural Prototypes

In an effort to understand SLA 3D printing limitations and the subsequent effects on critical design features, structural prototypes were created for the dog bone and reverse dog bone lattices, shown in Figure 5.2(a) and 5.2(b), and unit cells, shown in Figure 5.2(c).
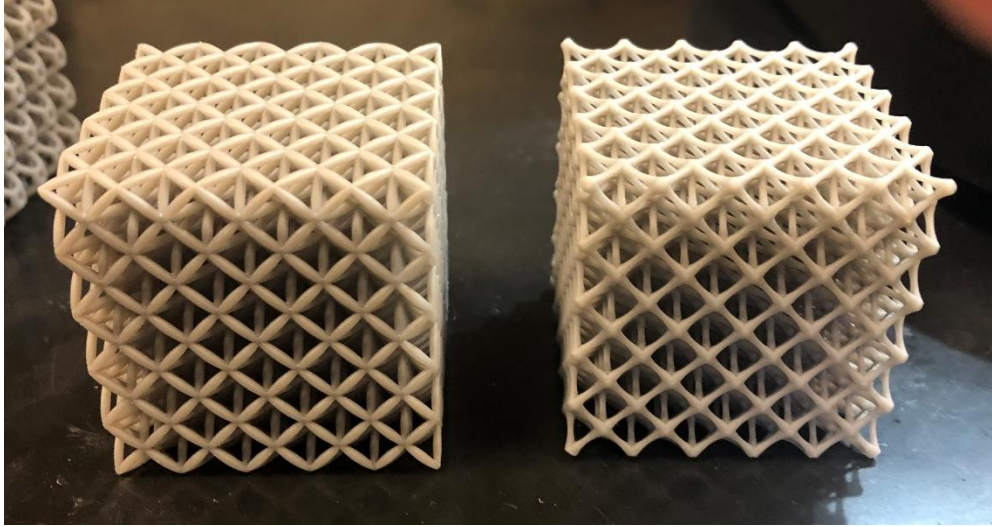
Figure 5.2(a). Reverse dog bone (left) and dog bone (right) lattice structural prototypes.
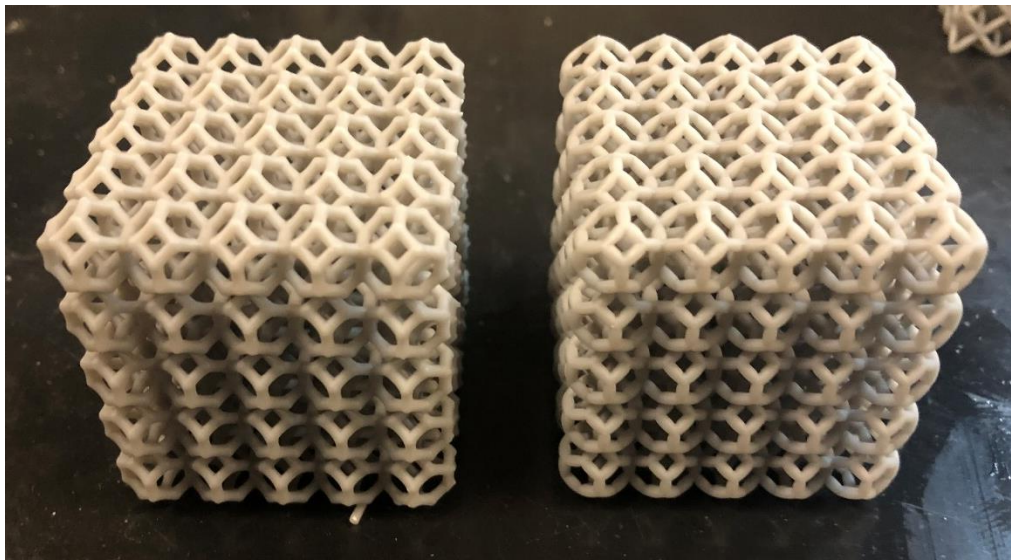
Figure 5.2(b). Dog bone (left) and reverse dog bone (right) lattice structural prototypes.

The print quality of the lattices depicted above exceeded expectations. It should be noted that a few iterations of print orientation and support configurations were attempted to arrive at this level of print quality. A key learning of initial "practice" prints was that particular strut designs require the lattices to be printed at an angle to prevent unsupported minima. Unsupported minima are floating or weakly anchored areas of a print layer that may break off the part during printing, leading to structural defects. This print angle is a significant factor that must be implemented across all the final test specimen prints in order to eliminate this as a causal variable in the material property outcomes of stress-testing.

During modeling, one objective was to keep the masses, and thus lattice densities, constant across the various strut designs. The specific requirement is a that the heaviest and lightest lattice masses are within 10% of each other. Solidworks® mass properties was implemented to carry out this requirement. A significant learning from the structural prototype was that, despite matching mass properties across models, the actual masses did not deliver consistent masses. Fortunately, the percent variation was consistent for several print sizes, as shown in Figure 5.2 9(c) and can be compensated for.
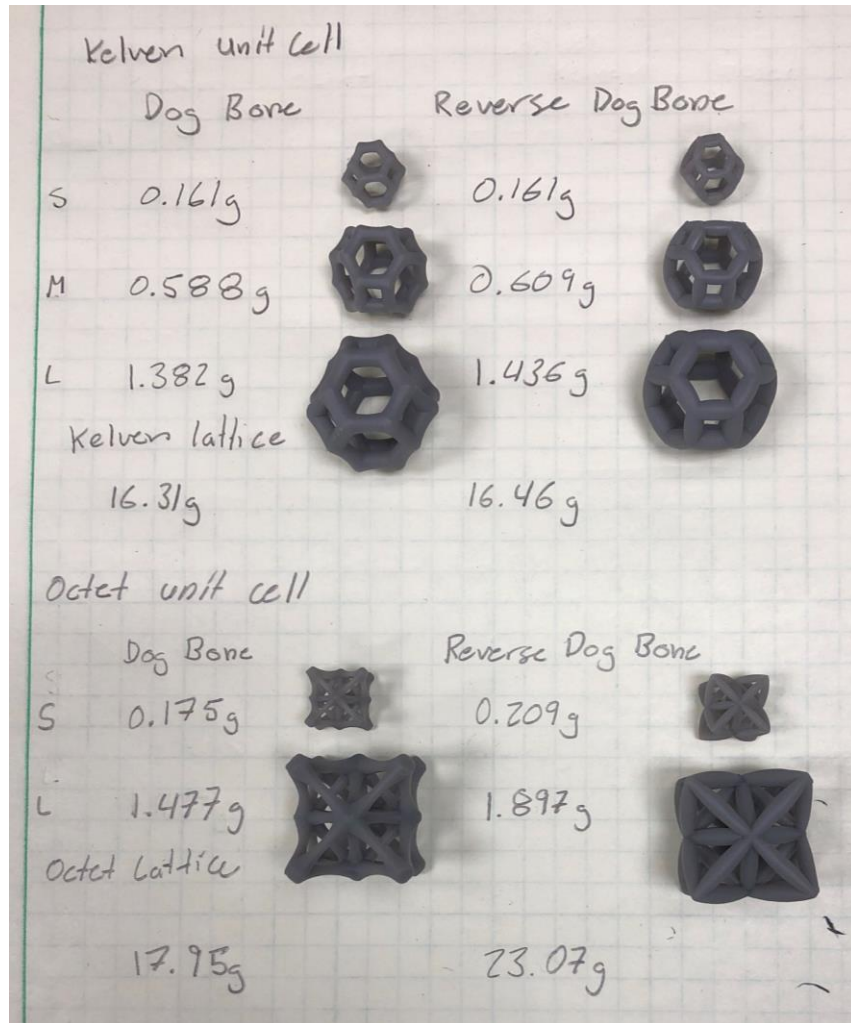
Figure 5.2(c). Unit cell structural prototypes with mass of each indicated.

5.3 Cost Analysis

The costs to carry out the manufacture of the final lattices are broken down in the indented bill of materials in Appendix E. The measurable material costs originate entirely from the SLA resin, which costs $149 per cartridge. Based on the volumes of the prints, the total resin cost is $71.58. Because this is a cost analysis for the production of the final design, this does not include resin to print prototypes.

It is also worth noting that the costs to run production processes, including 3D printing and curing, are not included as they are not accurately measurable. A Formlabs Form 3B+ and Form Cure are available for project use through Dr. Wang's research laboratory.

6. Manufacturing Overview

6.1 Procurement

The procurement of materials required for the fabrication of the team's lattices was achieved through grants secured by project sponsor Dr. Wang. This project requires the use of a high-quality 3D printer, in particular, an SLA printer, as many FDM printers are unable to produce the resolution and intricacy required. The printer used in this project is the Formlabs Form 3B+, along with the Form Cure curing oven, printing with both the Gray and Elastic 50A resins. These resins are purchased on the Formlabs website strictly to ensure print quality and consistency.

6.2 Manufacturing

To ensure consistent lattices, prints follow a specific protocol that has been developed through several phases of test print iterations. The following procedure is implemented for each lattice design:

Modeling. To 3D print structures for testing, .STL files are generated from solid models. These solid models were created using Solidworks®. During modeling, one objective was to keep the masses, and thus lattice densities, constant across the various strut designs. The specific requirement is that the heaviest and lightest lattice masses are within 10% of each other. Solidworks® mass properties evaluation was implemented to carry out this requirement. A significant learning from the structural prototype was that, despite matching mass properties across models, the actual masses after printing varied. In response, lattice models were iterated on to develop prints with the desired masses.

Pre-processing. The model is then supported using a custom support structure, with supports placed on every node facing the print bed. Notably, printing the reverse dog bone lattice in a vertical orientation results in unsupported minima throughout the lattice. Because print orientation affects directional material strength, all lattices must be printed in the same orientation. Rotating 45° about the y and z axis removes the unsupported minima in the reverse dog bone and does not introduce any unsupported minima in the other strut designs.

A typical preprocessed lattice is seen in Figure 6.1. It is important to note that while the red areas indicate an under supported print design, the repeating unit structure of the lattices printed allow for subsequent layers to support those above them, resulting in successful prints even with "under supported" locations.
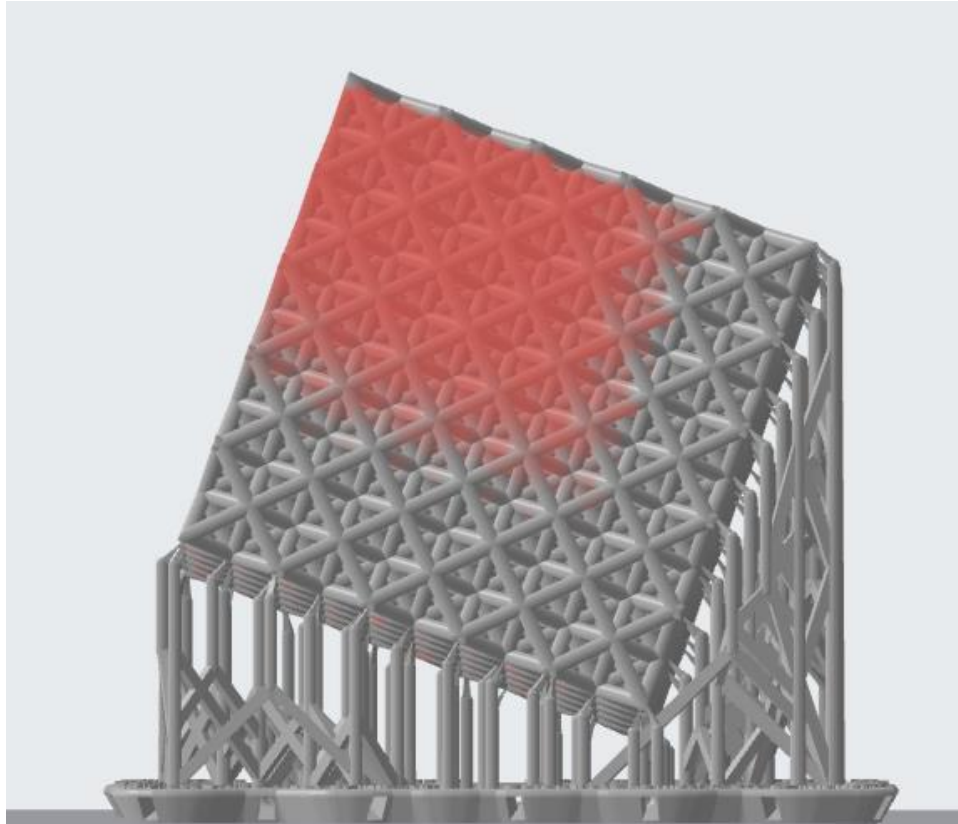
Figure 6.1. Supported Lattice in Preform.

Print. Form 3B+ is initialized, PreForm file loaded, and print carried out to completion.

Post-processing. Following the print, supports are carefully removed using wire cutters and a razor. The prints are subsequently washed in an isopropyl alcohol bath for 10 minutes, removing all uncured resin from the lattice. The final step is curing the prints in the Form Cure. Prints composed of gray resin require a cure time of 50 minutes at 60°C. Prints composed of elastic 50 A require a cure time of 20 minutes at 60°C.

7. Design Verification Overview

Table 3.1 housed in the Objectives section of this report outlines the specifications for this project. This section explains the approach to evaluation of whether the verification prototype meets these specifications.

7.1 Verification of Requirements

There are a few key requirements that the lattices must meet, as specified in the Problem Statement section. The overall lattice dimension must be less than 14cm x 14cm x 18.5cm. This can be easily measured with calipers. The three lattice density targets are 0.15, 0.20 and 0.25 g/cm^3, which is determined by dividing the mass of the lattice by the overall lattice volume. Additionally, given the number of distinct solid models needed, 3D modeling of the lattices must average no more than about an hour per design. The print time should be less than a day to allow new prints to be initialized on consecutive days. Finally, prediction of stresses within the test specimens is desired to facilitate understanding of the anticipated lattice performance during compressive testing. This is analyzed using Fusion 360 finite element analysis.

7.2 Compressive Testing

Ultimately, the goal of this project is to classify the behavior of various permutations of strut geometries, lattice types, and lattice densities. The key quantitative method of evaluation of lattice performance is compressive testing. The Instron located in the Materials Engineering laboratory is utilized for this test. A standard parallel plate fixture is employed for the compressive testing, and the rigid lattices are taken to complete failure (strain to fracture).

Additionally, qualitative classification of the compressive test results is desired to draw conclusions regarding causes for varying mode of failure (i.e. buckling, bending, shear, etc.). For this, high speed video enables retrospective failure analysis. Additionally, post-compressive inspection of fractured test coupons provides insight to failure mode and location.

7.3 Testing Results

1.2.SLA 3D Print Quality

Nominal values for lattice overall dimensions are shown and compared to the actual prints. The coefficient of variation $\left(\frac{Stamdard\ Deviation}{Mean}\right)$ based on ten strut midpoint thicknesses for each lattice are listed.

Table 7.1. Print quality.

	Overall Dimensions (L x W x H) [mm]		Strut Thickness
Lattice	Nominal	Actual	Coefficient of Variation
K-C-22.4	45.0 x 45.0 x 42.5	45.1 x 45.1 x 42.7	2.9%
K-C-26.9		45.1 x 45.1 X 42.5	1.1%
K-C-16.3		45.1 x 45.0 x 42.5	1.1%
K-D-23.6		45.0 x 45.1 x 42.6	1.1%
K-RD-21.6		44.9 x 45.0 x 42.5	2.2%
O-C-21.1	45.0 x 45.0 x 45.0	45.1 x 45.2 x 45.0	3.0%
O-C-26.9		45.1 x 45.2 x 45.0	3.0%
O-C-16.6		45.3 x 45.4 x 45.1	2.3%
O-D-21.9		45.0 x 45.2 x 45.1	2.3%
O-RD-22.9		45.0 x 45.3 x 45.2	2.4%

Finite Element Analysis

Finite element analysis of the different structures was conducted using the commercial software ABAQUS. Using the aforementioned Solidworks® models, additional plates were modeled and rigidly fixed to the top and bottom surfaces of the lattices as seen in Figure 7.1. These plates were used to model the compression seen on the lattices in the testing protocol. Three distinct boundary conditions were placed, the bottom plate saw zero degrees of freedom, the top plate was allowed displacement in the U2 direction, along the length of compression, and finally, the top plate was also set to displace the distance seen in the mechanical compression tests. As the computational requirements for solid elements can be quite intensive, a simplification of the model was required to complete this analysis. This reduction was achieved by cutting the models into quarters as seen in Figure 7.1. Along the XY face a Z directional boundary condition was placed, and along the ZY face a X directional boundary condition was placed. As these models are symmetric, these boundary conditions should play no role in the analysis of the model while dropping the required elements and run time for the simulations.

The top and bottom plate were modeled as steel, and the lattice was modeled using the mechanical properties provided by Formlabs for Gray resin. As only elastic modulus, elongation at break, and ultimate strength were provided, Gray resin was assumed to begin plastic deformation at 1% strain, as well as have a linear stress strain curve between yield and ultimate stress. To mesh the model, solid elements were used, meshing using the Tetrahedral elements.

Finally, to determine the required mesh sizes, a convergence analysis was performed, analyzing the ratio of max stress at the center node of the center unit cell, σ_n to the max stress seen in the adjacent structs to this center node, σ_s, referred to as the FEA stress ratio. Once the FEA stress ratio was changing by less than 10%, the given seed size was selected. The results of the convergence study for both the Kelvin and Octet lattices are seen in Tables 7.2 and 7.3.
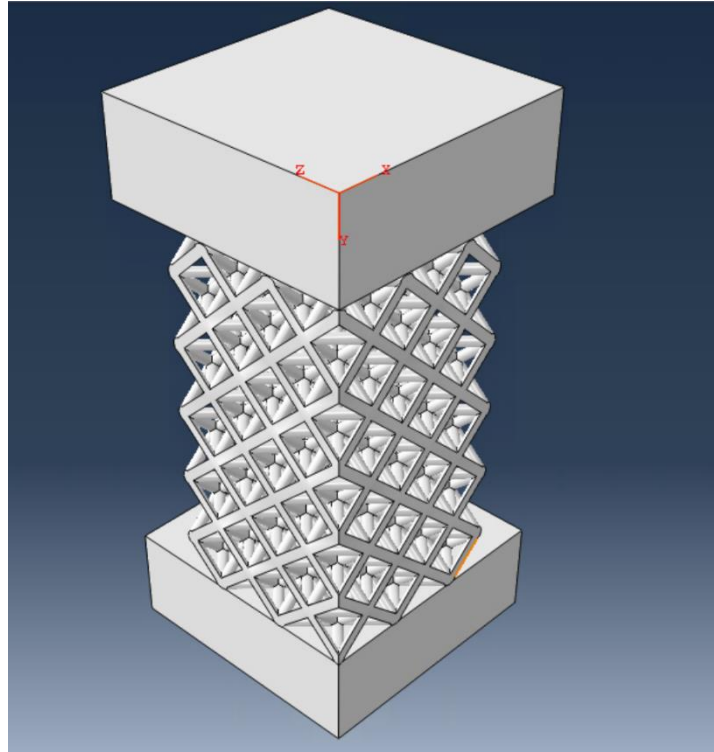
Figure 7.1. Reduced lattice model, one quarter of the entire structure. Coordinate system for the boundary conditions used located on the corner of the top plate.

The stress distribution in the two different lattices from the FEA are seen in Figure 7.2 and Figure 7.3. These results are for both the cylindrical and reverse dog bone strut structures, as the dog bone strut lattice was unable to be meshed.

Table 7.2. FEA convergence study results of cylindrical and reverse dog bone Kelvin lattice.

	Seed Size	Elements	Center Strut Stress, σ_s [MPa]	Center Node Stress, σ_n [MPa]	FEA stress Ratio, σ_n/σ_s	% Difference
K-C	8	46,761	19.7	38.7	2.0	
	6	76,155	16.3	36.6	2.3	14.7
	4	173,904	15.2	37.2	2.4	8.7
K-RD	8	50,253	13.1	36.4	2.8	
	6	84,658	12.2	36.4	3.0	7.8

Table 7.3. FEA convergence study results of cylindrical and reverse dog bone Octet lattice

	Seed Size	Elements	Center Strut Stress, σ_s [MPa]	Center Node Stress, σ_n [MPa]	FEA stress Ratio, σ_n/σ_s	% Difference
O-C	8	55,823	37.8	64.1	1.7	
	5	146,916	38.5	71.0	1.8	8.8
O-RD	8	55,823	26.0	67.3	2.6	
	6	146,916	24.8	68.9	2.8	7.5
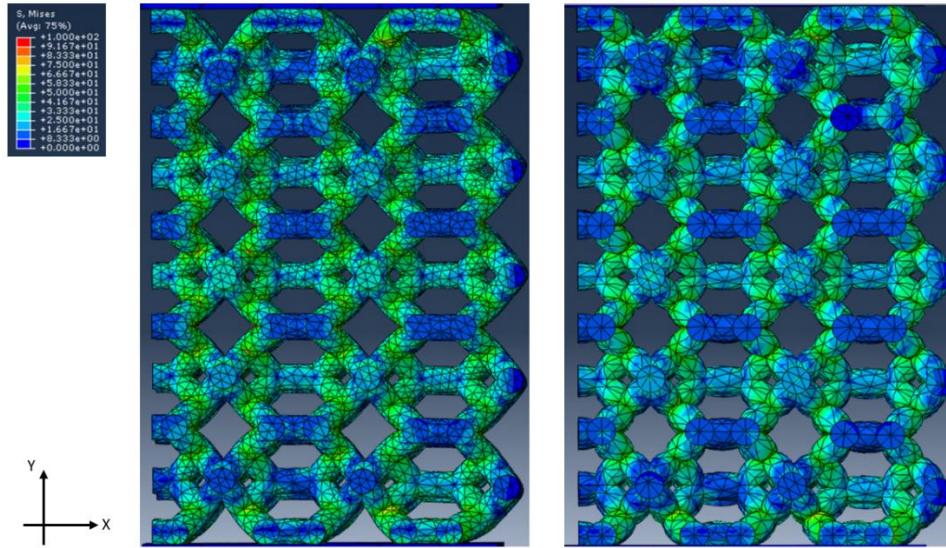
Figure 7.2. Von Mises FEA stress distribution in the cylindrical and reverse dog bond Kelvin lattices seen left to right.
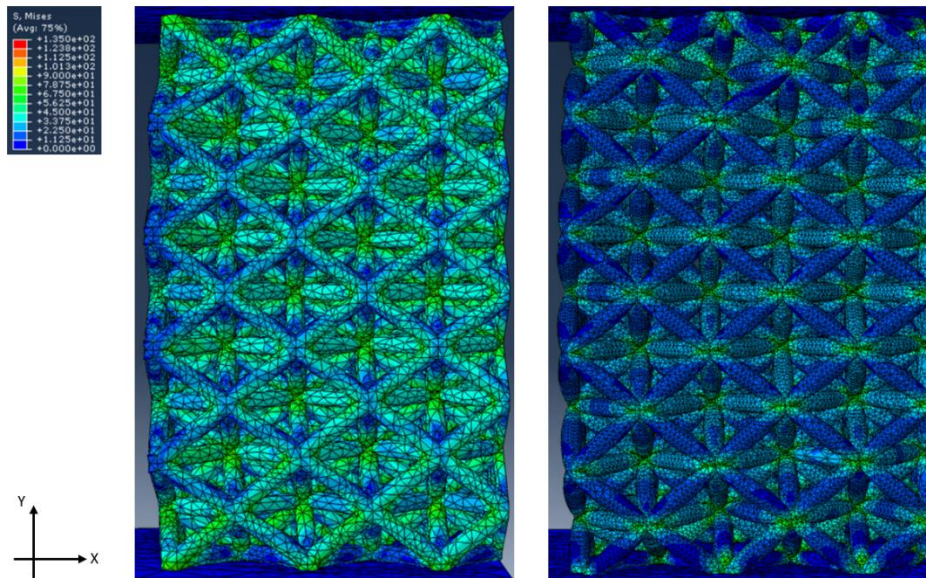
Figure 7.3. Von Mises FEA stress distribution in the cylindrical and reverse dog bond Octet lattices seen left to right.

Mechanical Testing

The graphs below display weighted stress [MPa] as a function of strain [-]. Strain is defined as $\frac{Displacement\,[mm]}{Undeformed\,Lattice\,Height\,[mm]}$. *Weighted stress is defined as* $\frac{Load\,[N]}{Cross-sectional\,Area\,[mm^2]} \cdot \frac{1}{\%\,Infill}$. This value factors in the mass differences between lattices, allowing the compressive testing results to be a result of mass placement.
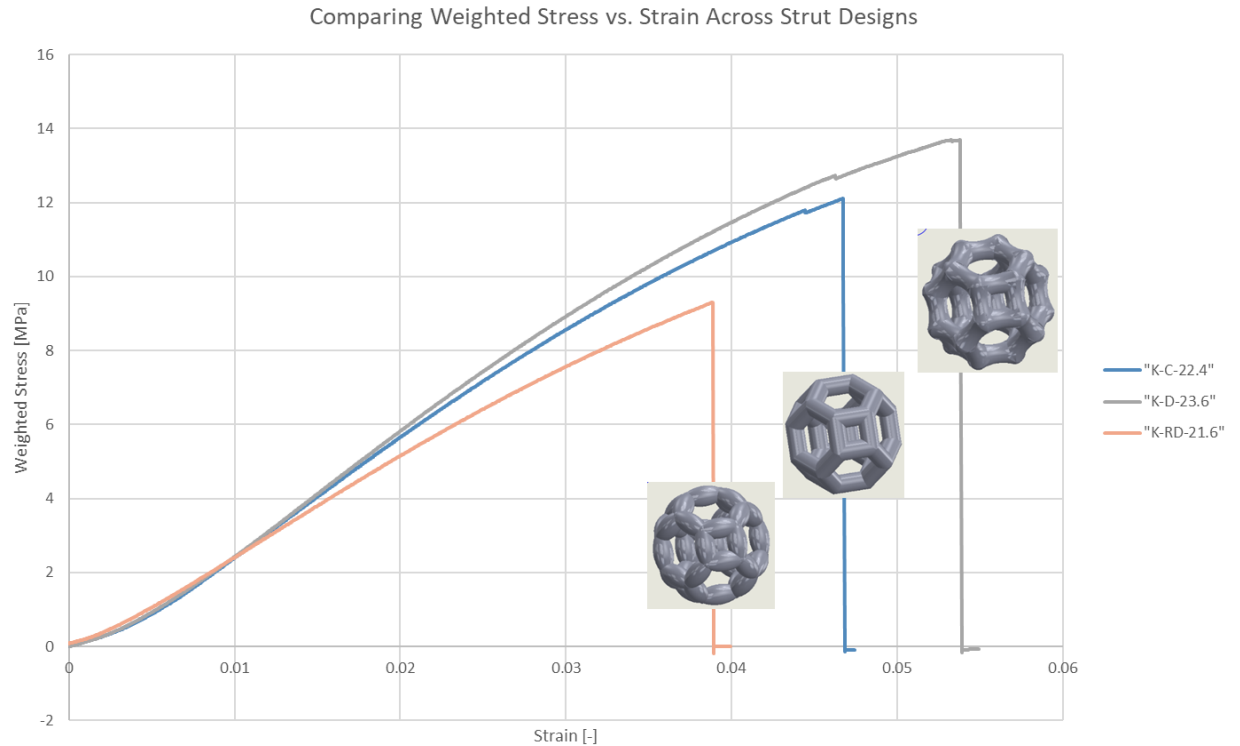
Figure 7.4. Weighted stress plotted as a function of strain for kelvin cell with various strut geometries.
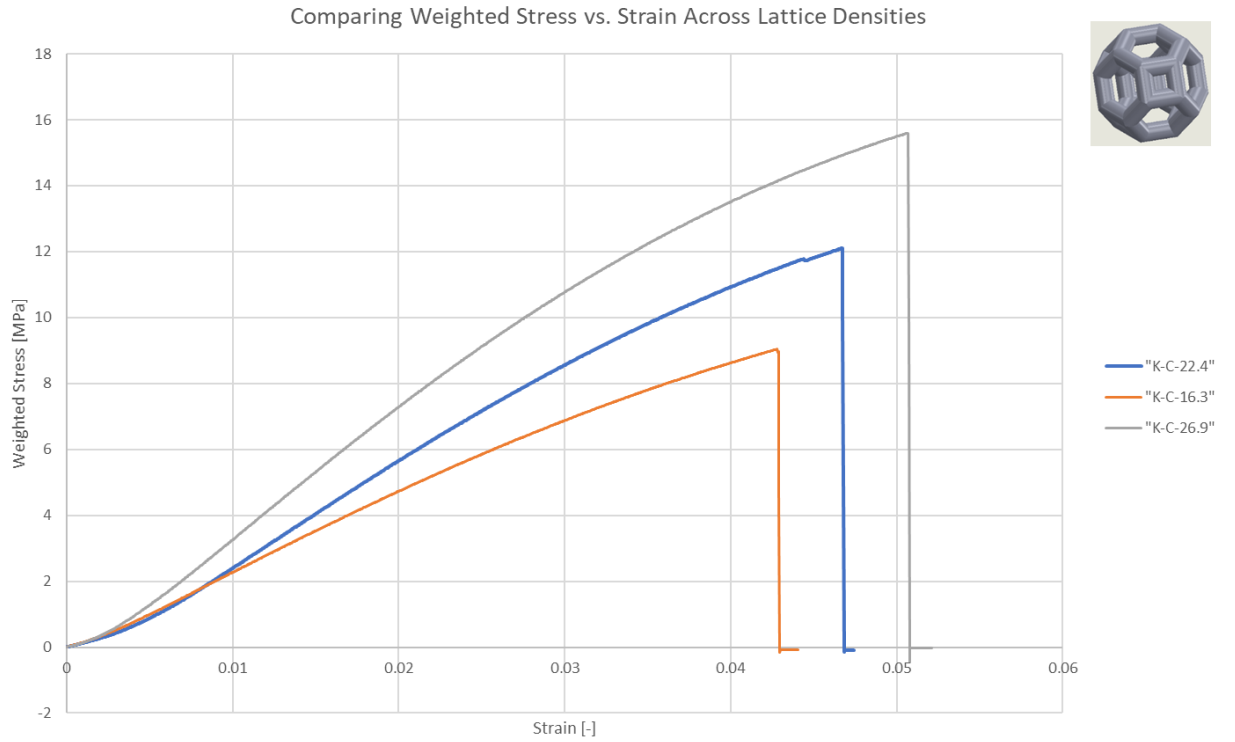
Figure 7.5. Weighted stress plotted as a function of strain for kelvin cell with various masses.
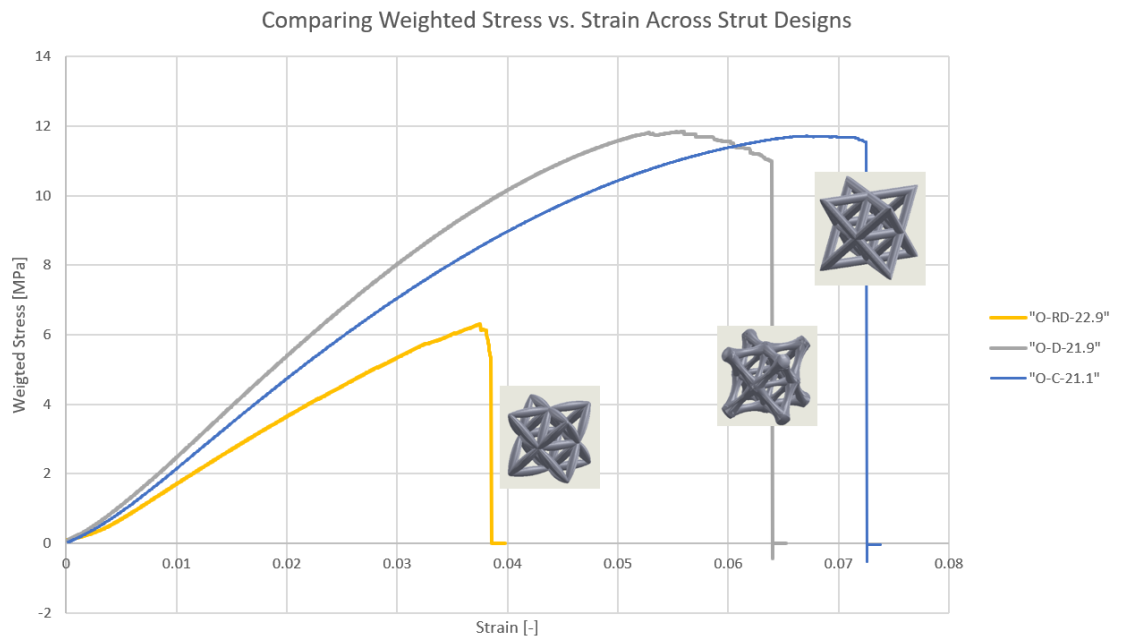
Figure 7.6. Weighted stress plotted as a function of strain for octet truss with various strut geometries.
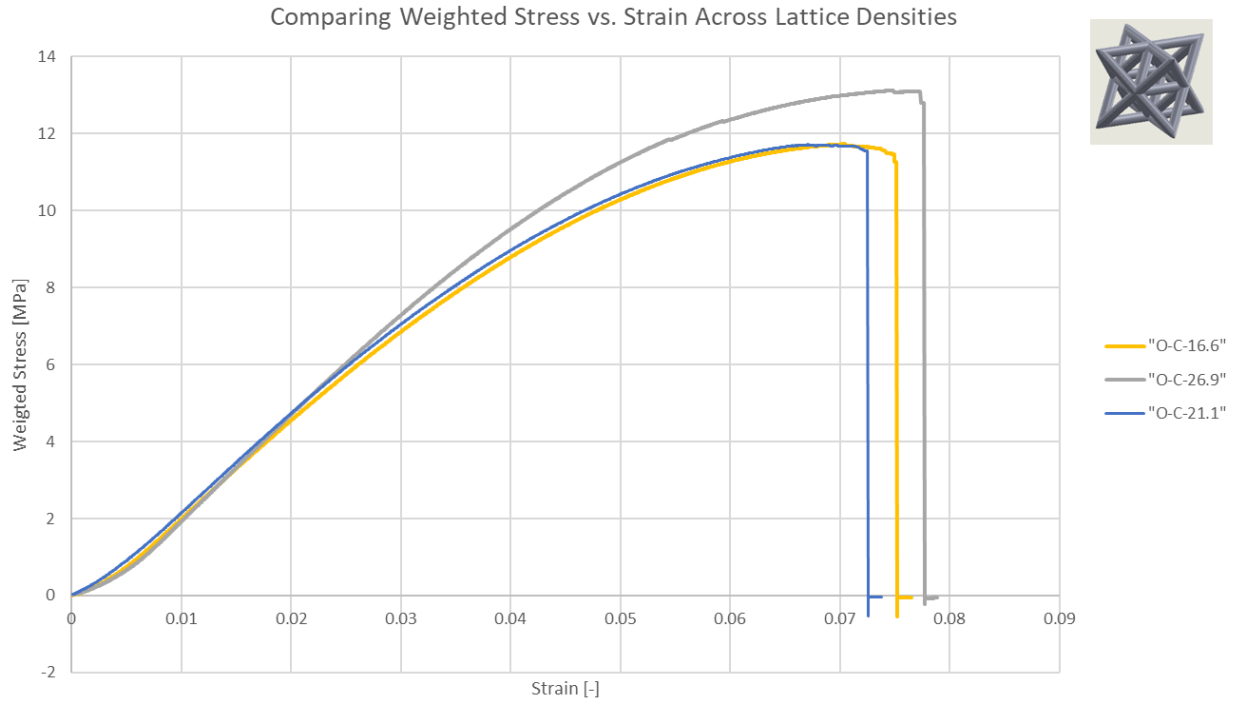
Figure 7.7. Weighted stress plotted as a function of strain for octet truss with various masses.

7.4 Discussion

SLA 3D Print Quality

The print outcomes listed in Table 7.1 show that the actual dimensions of all lattice prints are very close to the as-modeled nominal dimensions. The largest observed discrepancy in any single overall dimension is 0.4 mm: approximately 0.9% off-target. In addition to overall lattice dimensions, variation in strut thicknesses within each lattice was assessed. Included in Table 1, the coefficients of variation for strut thicknesses fall between 1% and 3%. Together, overall dimension measurements and strut thickness variations demonstrate exceptional SLA 3D print quality outcomes.

Finite Element Analysis

As seen in Figure 7.2, the mesh refinement in the reverse dog bone Octet lattice is much finer than the cylindrical lattice, due to the curved nature of the struts intersecting at the nodal locations, making accurate meshing difficult. To compensate for this and enable meshing, mesh controls were changed for this lattice, resulting in the large number of elements seen in Table 7.2. This is not seen however for the Kelvin cell, as at the nodal locations there are fewer structs intersecting and meshes were able to be generated that required less elements.

Evaluating the Kelvin lattices, as the material leaves the nodes and the struts go from cylindrical to reverse dog bone, the stress begins to localize in the nodal locations, however this change in distribution is not dramatic. As seen in Table 7.3, the change in the FEA stress ratio of σ_n to σ_s does not alter greatly between in two different strut designs, though for both strut designs the value

21

is relatively high. Additionally, this agrees with what was seen in our mechanical testing, as seen in Figure 7.8(b), as the reverse dog bone lattice fails in a similar manner to that of the dog bone structure, with failures occurring slightly more commonly at the nodal locations.

Figure 7.2 shows the FEA results of the Octet cell with both cylindrical and reverse dog bone struts. The difference between these two strut designs is much more pronounced than what was seen in the Kelvin cell, reflected in both the stress distribution and the FEA stress ratio. This change in stress distribution is also seen in our mechanical testing, with the reverse dog bone structure exhibiting complete nodal failure where every strut broke off cleanly at a node.

Mechanical Testing

Figures 4 through 7 display weighted stress, defined in section 2.3, as a function of strain. From Figure 4, it is observed that moving mass to the nodes of the Kelvin cell (i.e dog bone strut) results in increased structure strength. Similarly, moving mass away from the nodes reduces the strength of the structure when compared to a standard cylindrical strut geometry. For the bending-dominated Kelvin cell, nodal failure is expected under compression and can be observed in the post-failure lattice images of figures 7.8(a) and 7.8(b). As such, a node-favored material distribution was both expected and observed to support a greater load.
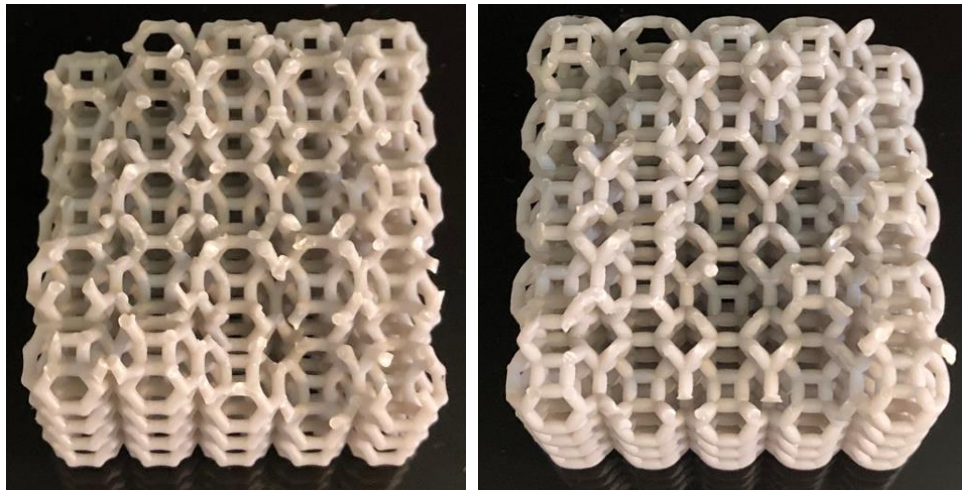
Figure 7.8(a). Dog bone Kelvin cell after failure. Nodal failure observed.

Figure 7.8(b). Reverse dog bone Kelvin cell after failure. Nodal failure observed.

Figure 5 compares the effects of changing lattice mass alone. A cylindrical strut geometry is maintained across three different masses: nominal, +25%, and -25%. Weighted stress provides a first-order correction for differences in mass. Significant weighted stress differences are observed for this wide range of masses, indicating that the relationship between lattice strength and lattice mass within a kelvin-cell configuration is non-linear. An increase in strut thickness implies an increase in material at the lattice nodes, resulting in the non-linear increase cylindrical lattice mass and peak stress.

The relationship between weighted strength and strain of the octet truss lattices with varying strut geometries is observed in figure 7.5. Again, it is clear that the reverse dog bone structure remains the weakest. The cylindrical and dog bone structures display very similar points of failure. The dog bone octet truss has a greater elastic modulus, indicated by the slope of the linear region of the weighted stress vs. strain curve, and fails under a smaller amount of deformation. In other words, the dog bone stretch-dominated structure displayed more rigid behavior compared to a cylindrical configuration.

In contrast to the kelvin cell lattice failure, the octet truss structures display planar failure. Failure in the dog bone structure, shown in figure 7.9(a), generally occurs at the strut midpoints. Failure in the reverse dog bone structure occurs almost entirely at the nodes. These failure modes are consistent with one another, as the location of failure in both cases is the location of smallest beam diameter. This outcome is consistent with expectations for a structure that favors axial loading.
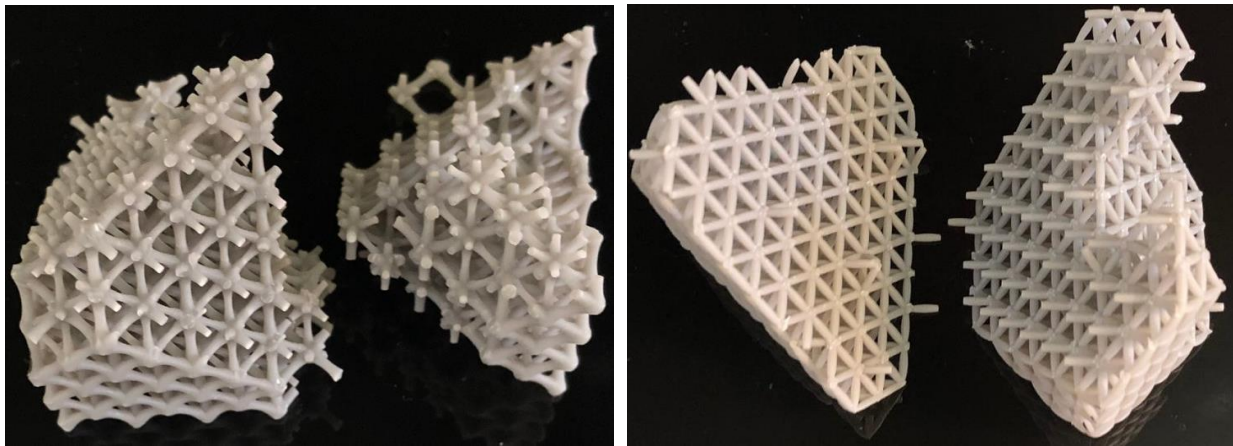
Figure 7.9(a). Dog bone octet truss after failure.

Figure 7.9(b). Reverse dog bone octet truss after failure. Nodal failure observed.

When evaluating the effects of increasing octet truss mass without changing strut geometry, weighted stress does not vary significantly with overall lattice mass. Unlike the Kelvin cell structures, the relationship between non-weighted stress and lattice mass behaves linearly within the range of masses tested. This observation is consistent with expectations based on the axial load distribution characteristic of the octet truss, where stress within a strut has a first order inverse relationship to the strut's cross-sectional area.

8. Project Management

The design process for this project can be classified into three main stages: design, build, and testing. Each of these stages align with consecutive quarters of the Cal Poly academic calendar. Table 8.1 highlights the dates corresponding to major deliverables over the three quarters: Spring 2022, Fall 2022, and Winter 2023.

Table 8.1. Major senior project deliverables.

Deliverable	Date
Statement of Work	April 28, 2022
Preliminary Design Review	May 26, 2022
Critical Design Review	October 27, 2022
Manufacturing & Test Review	December 6, 2022
Verification Prototype Sign-off	January 10, 2023
Final Design Review	March 17. 2023

These major deliverables are accomplished by means of sequential completion of more focused individual tasks. For example, the statement of work is a product of initial an initial research stage aimed entirely at gaining an understanding of the current state of the metamaterials body of research. Information regarding lattice types, applications, and manufacturing techniques were researched and documented. In addition, due to the broad array of applications of structural metamaterials, project objectives were narrowed to those listed in the "Objectives" section of this document. The Gantt chart contained in appendix A lays out the timeline of the major deliverables listed above in addition to the smaller tasks that contribute to the larger project milestones.

8.1 General Process Plans

The design process for this project was initiated by preliminary research into several aspects necessary to the success of this project. Beyond knowledge of lattice and cell types, research into the existing modeling and manufacturing strategies was required. In other words, the team is tasked with unit cell selection and modeling, propagation of unit cell into lattice structure, precision manufacturing of this lattice structure, and ultimately testing. This research aided the team in the selection of appropriate unit cells for study as well as modeling and prototyping. Further, the design phase was also where the team narrowed the scope of the project: creation and testing of one bending-dominated and one stretch-dominated lattice with both standard cylindrical struts as well as dog bone struts at various thicknesses to evaluate the effects of strategic placement of mass within a lattice structure. See the concept creation chapter of this report for more information.

The second stage of the design process is the build phase. For this project, this entails the creation of 3D solid models which are then processed and printed using SLA 3D printing. The build phase necessitates that a reliable modeling procedure be created and that the lattice SLA prints are both high in quality and repeatable.

The last major phase of this design project is the testing phase. For this phase, the plan was to implement a quasistatic compression test on the lattices printed with the acrylic resin at the various strut thicknesses of interest. This is performed for cylindrical, dog bone, and reverse dog bone struts. The max stress is then plotted as a function of relative density for each strut design and each

stress distribution mode (bending or stretch). This provides a basis for data analysis to create conclusions of the effects of mass placement on the strength of 3D metamaterials. The Instron universal tester in the MATE department is employed for this compressive testing.

9. Conclusions and Recommendations

The results of compressive testing demonstrate differences in mechanical properties between lattice configurations. A comprehensive review of the results and discussion can be found in section 7 of this report.

While the observations of this report are significant and serve as a foundation for future research, the conclusions of this work are limited by the unclear effect of statistical variation. To understand the typical variation to be expected between identical lattice structures, future tests should include multiple trials of identical structures.

Additionally, the team is interested in performing a similar structural analysis on elastic lattices. Lattices of this type will be printed FormLabs Elastic 50a resin. Elastic structures will be tested under dynamic loading instead of the quasistatic compression implemented for testing of the inelastic lattices.

10. References

[1] A.H Azman 1, F.Vignat 1, F. Villeneuve 1. *Evaluating Current CAD tools Performance in the Context of Design for Additive Manufacturing,* 2014

[2] Julien Favre, Paul Lohmuller, Boris Piotrowski, Samuel Kenzari, Pascal Laheurte, et al.. *A continuous crystallographic approach to generate cubic lattices and its effect on relative stiffness of architectured materials*. Additive Manufacturing, Elsevier, 2018, 21, pp.359-368

[3] Oraib Al-Ketan, Rashid K. Abu Al-Rub. *MSLattice: A free software for generating uniform and graded lattices based on triply periodic minimal surfaces,* 2020

[4] V. S. DESHPANDE, M. F. ASHBY, N. A. FLECK. *Foam Topology Bending Versus Stretching Dominated Architectures.* Acta mater. 49 (2001) pp. 1035–1040

[5] Tobias Maconachie , Martin Leary, Bill Lozanovski, Xuezhe Zhang, Ma Qian, Omar Faruque, Milan Brandt. *SLM lattice structures: Properties, performance, applications and challenges.* Materials and Design 183 (2019)

11. Appendices

11.1 Appendix A – Gantt Chart

11.2 Appendix B – House of Quality

Correlations

Positive	+
Negative	–
No Correlation	

Relationships

Strong	●
Moderate	○
Weak	▽

Direction of Improvement

Maximize	▲
Target	◇
Minimize	▼

QFD House of Quality

Project: Mechanical Metamaterials

Revision Date: 04/21/2022

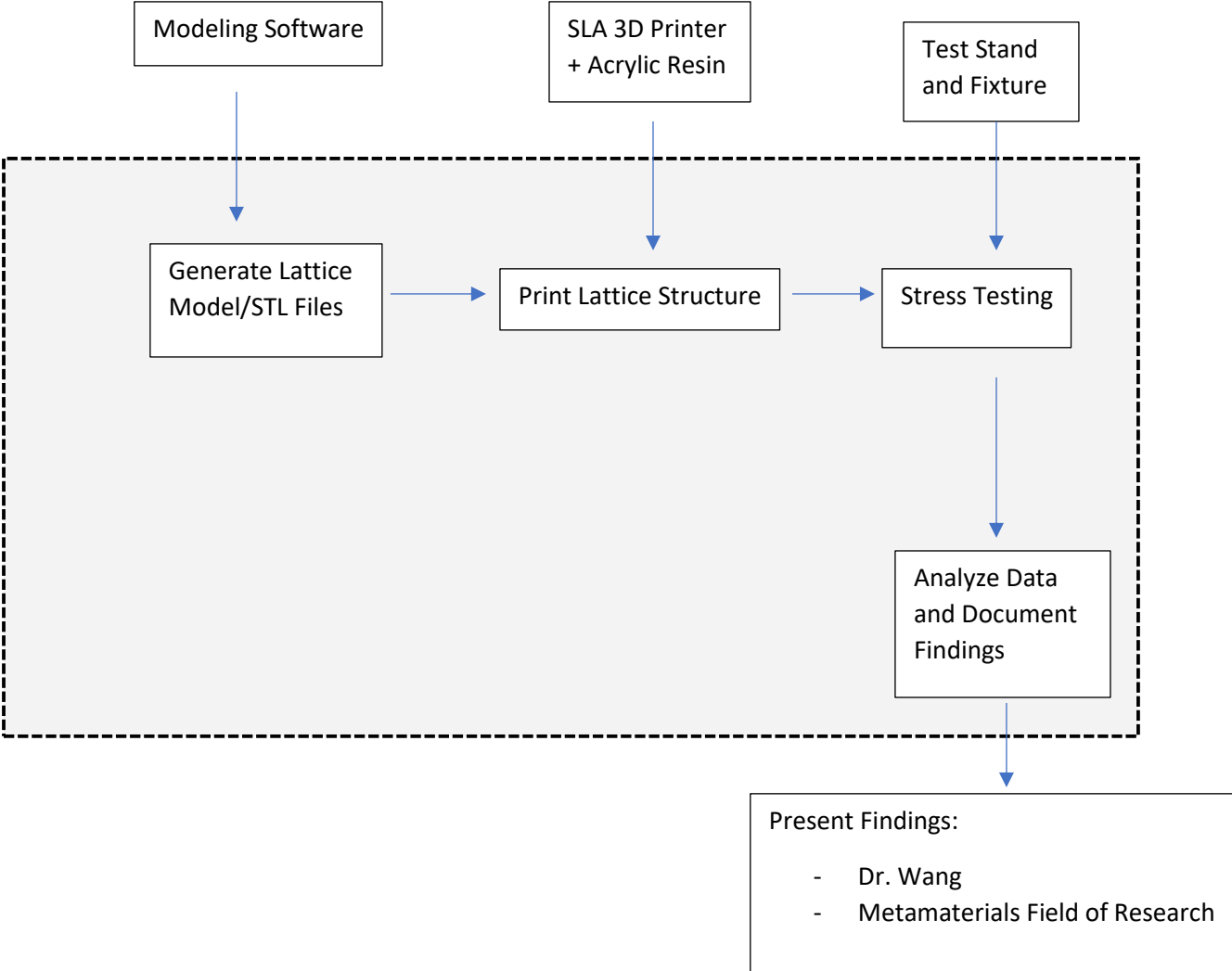| Row #	Weight Chart	Relative Weight	Dr. Wang	Dr. Wang's Research Group	Metamaterials Field of Research	Maximum Relationship	WHAT: Customer Requirements (Needs/Wants)	Crush Test	Time to Print	Stress-Strain Curve	Energy Absorbed	Production Cost	Size	Finite Element Analysis	Time to Model	Competitor #1: Lohmuller et al.	Competitor #2: Hadi et al.	Competitor #3: Han et al.	Row #
	Column #							1	2	3	4	5	6	7	8				
	Direction of Improvement							◇	▼	◇	▲	▼	◇	◇	▼				
1	▬	16%	7	7	2	3	SLA 3D Printed		○							0	0	0	1
2	▬	17%	8	4	4	9	Vary Single Lattice Parameter	●		●	●				●	0	0	0	2
3	▮	9%	5	3	1	3	Use of Acrylic Resin	○		○	○			○		1	0	0	3
4	▬	20%	6	6	5	9	High Print Resolution		●							2	0	2	4
5	▮	7%	2	2	2	9	Inexpensive					●				1	0	2	5
6	▬	18%	5	7	4	9	Replicable 3D Model Generation		○			○		○	●	1	1	1	6
7	▬	13%	9	4	1	9	Within Max Printer Dimensions		○			○	●			1	0	2	7
8		0%																	8
9		0%																	9
10		0%																	10
11		0%																	11
12		0%																	12
13		0%																	13
14		0%																	14
15		0%																	15
16		0%																	16

WHO: Customers — Dr. Wang, Dr. Wang's Research Group, Metamaterials Field of Research

NOW: Curr. Products — Competitor #1: Lohmuller et al., Competitor #2: Hadi et al., Competitor #3: Han et al.

HOW MUCH: Target Values

	Crush Test	Time to Print	Stress-Strain Curve	Energy Absorbed	Production Cost	Size	Finite Element Analysis	Time to Model								
Target Values	Complete	Within 1 day	Complete	Complete	Within Wang's Budget	14.5 × 14.5 × 18.5 cm	Complete	1-2 hours per lattice								
Max Relationship	9	9	9	9	9	9	3	9								
Technical Importance Rating	182.9	317.7	182.9	182.9	157	116.4	80.43	319.2	0	0	0	0	0	0	0	0
Relative Weight	12%	21%	12%	12%	10%	8%	5%	21%	0%	0%	0%	0%	0%	0%	0%	0%
Competitor #1: Lohmuller et al.	3	2	3	1	2	3	3	1								
Competitor #2: Hadi et al.	3	2	3	1	1	3	3	1								
Competitor #3: Han et al.	3	2	3	1	1	3	3	1								
Column #	1	2	3	4	5	6	7	8	9	10	11	12	13	14	15	16

11.3 Appendix C – Boundary Sketch

Modeling Software

SLA 3D Printer + Acrylic Resin

Test Stand and Fixture

Generate Lattice Model/STL Files → Print Lattice Structure → Stress Testing → Analyze Data and Document Findings

Present Findings:

- Dr. Wang
- Metamaterials Field of Research

11.4 Appendix D – Design Hazard Checklist

Description of Hazard	Planned Corrective Action	Planned
Liquid SLA Resin can cause irritation in the case of eye contact or allergic reaction in the case of skin contact	Always use gloves and safety glasses when handling liquid resin. To remove resin from skin, wash thoroughly with soap and water. Do not wash skin with products containing alcohol, like hand sanitizer, or any other solvents.	During Printer Setup/Cleanup
Isopropyl alcohol is a highly-volatile, flammable, colorless, clear liquid with a strong smell. It is readily absorbed through the skin.	Handle IPA with gloves and eye protection. Avoid inhaling large amounts of IPA fumes.	During Printer Setup/Cleanup
Compressive testing on Instron can cause injury if operated incorrectly.	Training is required for Instron operators. Adequate PPE, including safety glasses, long pants, and long sleeves are required.	28 October 2022

11.5 Appendix E – Indented Bill of Material (iBOM)

Part Number	Descriptive Part Name				Qty	Mat'l Cost	Production Cost	Total Cost	Material Source	More Info
	Lvl0	*Lvl1*	*Lvl2*	*Lvl3*						
1000	Octet Truss									
1100		Cylindrical Struts								
1110			Unit Cell		1	$ 0.75	------	$ 0.75		
1120			3D Lattice							
1121				Low Relative Density	1	$ 2.98	------	$ 2.98	Formlabs	SLA 3D Printed
1122				Mid Relative Density	1	$ 3.73	------	$ 3.73	Formlabs	SLA 3D Printed
1123				High Relative Desity	1	$ 4.47	------	$ 4.47	Formlabs	SLA 3D Printed
1200		Dog Bone Struts								
1210			Unit Cell		1	$ 0.75	------	$ 0.75		
1220			3D Lattice							
1221				Low Relative Density	1	$ 2.98	------	$ 2.98	Formlabs	SLA 3D Printed
1222				Mid Relative Density	1	$ 3.73	------	$ 3.73	Formlabs	SLA 3D Printed
1223				High Relative Desity	1	$ 4.47	------	$ 4.47	Formlabs	SLA 3D Printed
1300		Reverse Dog Bone Struts								
1310			Unit Cell		1	$ 0.75	------	$ 0.75		
1320			3D Lattice							
1321				Low Relative Density	1	$ 2.98	------	$ 2.98	Formlabs	SLA 3D Printed
1322				Mid Relative Density	1	$ 3.73	------	$ 3.73	Formlabs	SLA 3D Printed
1323				High Relative Desity	1	$ 4.47	------	$ 4.47	Formlabs	SLA 3D Printed
2000	Kelvin Cell									
2100		Cylindrical Struts								
2110			Unit Cell		1	$ 0.75	------	$ 0.75		
2120			3D Lattice							
2121				Low Relative Density	1	$ 2.98	------	$ 2.98	Formlabs	SLA 3D Printed
2122				Mid Relative Density	1	$ 3.73	------	$ 3.73	Formlabs	SLA 3D Printed
2123				High Relative Desity	1	$ 4.47	------	$ 4.47	Formlabs	SLA 3D Printed
2200		Dog Bone Struts								
2210			Unit Cell		1	$ 0.75	------	$ 0.75		
2220			3D Lattice							
2221				Low Relative Density	1	$ 2.98	------	$ 2.98	Formlabs	SLA 3D Printed
2222				Mid Relative Density	1	$ 3.73	------	$ 3.73	Formlabs	SLA 3D Printed
2223				High Relative Desity	1	$ 4.47	------	$ 4.47	Formlabs	SLA 3D Printed
2300		Reverse Dog Bone Struts								
2310			Unit Cell		1	$ 0.75	------	$ 0.75		
2320			3D Lattice							
2321				Low Relative Density	1	$ 2.98	------	$ 2.98	Formlabs	SLA 3D Printed
2322				Mid Relative Density	1	$ 3.73	------	$ 3.73	Formlabs	SLA 3D Printed
2323				High Relative Desity	1	$ 4.47	------	$ 4.47	Formlabs	SLA 3D Printed
Total Parts					**24**			**$ 71.58**		
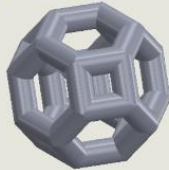
11.6 Appendix F – Design Verification Plan

DVP&R - Design Verification Plan (& Report)											
Project:	Mechanical Metamaterials			Sponsor:	Long Wang					Edit Date:	10/11/2022
TEST PLAN										**TEST RESULTS**	
Test #	Specification	Test Description	Measurements	Acceptance Criteria	Required Facilities/Equipment	Parts Needed	Responsibility	TIMING		Numerical Results	Notes on Testing
								Start date	Finish date		
1	1	Verify that masses of prints are within 10% across the different strut geometries for each given relative density.	Masses of corresponding prints	Max and Min masses within 10%	Digital Scale	All unit cells and lattices	Oliver	10/13/2022			
2	2	Verify visually that the structure looks as intended with little to no residual resin, especially at structure nodes.	Visual Inspection	No noticeable deformations or extraneous resin buildup	NA	All unit cells and lattices	Oliver	10/13/2022			
3	3	Compressive test to generate stress-strain curves for each unit cell and lattice configuration.	Stress,. strain and high speed video	NA	Instron and parallel plate fixture	All unit cells and lattices	Brent/Oliver	10/24/2022			

32

11.7 Appendix G – Drawing Package

NOTES:
1. CYLINDRICAL STRUTS
2. DOG BONE STRUTS
3. REVERSE DOG BONE STRUTS
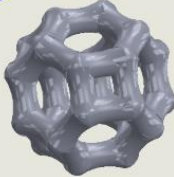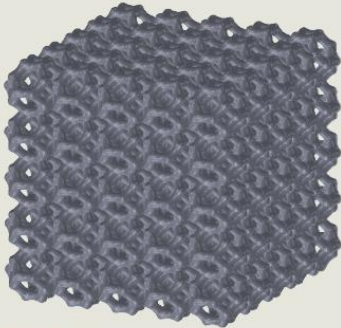
① SCALE: 4:1   ② SCALE: 4:1   ③ SCALE: 4:1
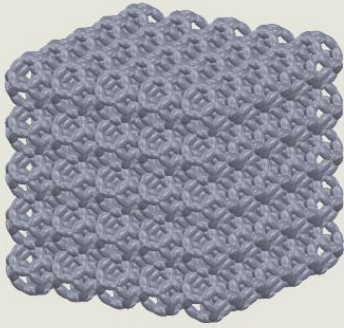
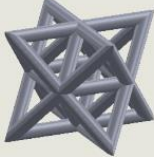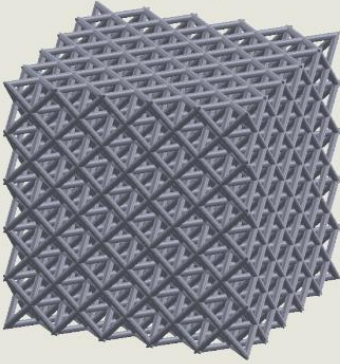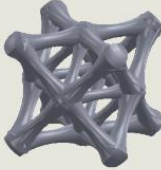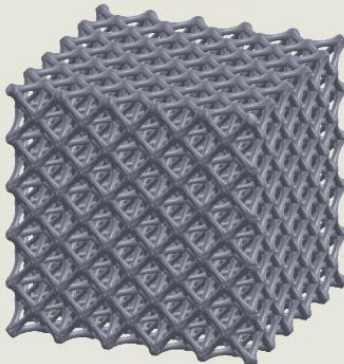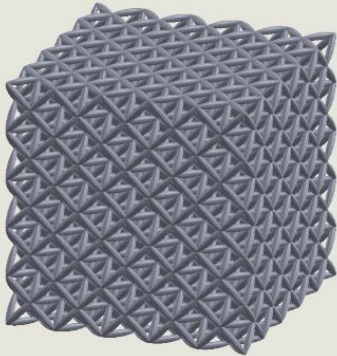SCALE: 3:2   SCALE: 3:2   SCALE: 3:2

UNLESS OTHERWISE SPECIFIED:
DIMENSIONS ARE IN INCHES
TOLERANCES:
ONE PLACE DECIMAL ± .1
TWO PLACE DECIMAL ± .01
THREE PLACE DECIMAL ± .005

INTERPRET DRAWING
PER ASME Y14.5 2009

CAL POLY
Mechanical Engineering
COLLEGE OF ENGINEERING

MATERIAL:
FORMLABS GRAY

TITLE:
KELVIN CELL UNIT CELLS AND LATTICES

DATE:
11 OCTOBER 2022

DRAWN BY:
BRENT PELUSO

SHEET 1 OF 1

REV
A

SIZE
A

SOLIDWORKS Educational Product. For Instructional Use Only.

11.7 Appendix G – Drawing Package Cont.

NOTES:
1. CYLINDRICAL STRUTS
2. DOG BONE STRUTS
3. REVERSE DOG BONE STRUTS

(1) SCALE: 4:1   (2) SCALE: 4:1   (3) SCALE: 4:1

SCALE: 3:2   SCALE: 3:2   SCALE: 3:2

| UNLESS OTHERWISE SPECIFIED: | INTERPRET DRAWING PER ASME Y14.5 2009 | CAL POLY Mechanical Engineering COLLEGE OF ENGINEERING | MATERIAL: FORMLABS GRAY | TITLE: OCTET TRUSS UNIT CELLS AND LATTICES | | |
| DIMENSIONS ARE IN INCHES TOLERANCES: ONE PLACE DECIMAL ± .1 TWO PLACE DECIMAL ± .01 THREE PLACE DECIMAL ± .005 | DATE: 11 OCTOBER 2022 | | DRAWN BY: BRENT PELUSO | SHEET 1 OF 1 | REV A | SIZE A |

SOLIDWORKS Educational Product. For Instructional Use Only.